an average of about three degrees. Not only is this effect, then, substantially less than the divergences exhibited in Fig. 2, but, more importantly, the effect would be the same for both entrance channels and thus could not cause the difference that is observed between them.

A more complete analysis of this problem, in which the behavior of fissioning nuclei in a particular narrow region of high spin is described in Ref. 2, requires the determination of the cross section for compound-nucleus formation in the various entrance channels. Such an investigation is presently underway.

ACKNOWLEDGMENTS

The authors wish to thank Montclair State College students M. Franko, J. Rolak, D. Voigtlander, and R. Wood for their help in analyzing the experimental results.

*Work supported by the U. S. Atomic Energy Commission.

†National Science Foundation Predoctoral Trainee.

‡Present address: Department of Chemistry, U.A.R. Atomic Energy Commission, Inshass, U.A.R.

[1]H. C. Britt and A. R. Quinton, Phys. Rev. 120, 1768 (1960).

[2]L. Kowalski, A. M. Zebelman, J. M. Miller, G. F. Herzog, and R. C. Reedy, Phys. Rev. 1, 259 (1970).

[3]I. Halpern and V. M. Strutinski, in *Proceedings of the Second United Nations International Conference on the Peaceful Uses of Atomic Energy, Geneva, 1955* (United Nations, New York, 1958), Vol. 15, p. 398.

[4]T. Sikkeland, A. E. Larsh, and G. E. Gordon, Phys. Rev. 123, 2112 (1961).

[5]V. E. Viola, Jr., and T. Sikkeland, Phys. Rev. 130, 2044 (1963).

[6]R. C. Reedy, Ph.D. thesis, Columbia University, 1969 (unpublished).

PHYSICAL REVIEW C VOLUME 3, NUMBER 3 MARCH 1971

# Gamma-Ray Studies of the Decays of $Xe^{142}$, $Cs^{142}$, $Ba^{142}$, and $La^{142}$†

J. T. Larsen,* W. L. Talbert, Jr., and J. R. McConnell

*Institute for Atomic Research and Department of Physics, Iowa State University, Ames, Iowa 50010*

(Received 4 November 1970)

Measurements are reported for $\gamma$-ray energies and intensities present in the $\beta$ decays of four nuclei $Xe^{142}$, $Cs^{142}$, $Ba^{142}$, and $La^{142}$. These nuclei are all members of the isobaric decay chain beginning with $Xe^{142}$, which was made available by use of an on-line isotope separator developed for the study of gaseous fission products. Partial energy level schemes have been constructed for $Cs^{142}$, $Ba^{142}$, $La^{142}$, and $Ce^{142}$ with the aid of Ge(Li)-Ge(Li) coincidence data. Some spin-parity assignments were made and relative transition probabilities determined for levels in $Ba^{142}$ and $Ce^{142}$; comparative half-lives were calculated for the decays of $Ba^{142}$ and $La^{142}$. The energy level scheme of $Ce^{142}$ suggests vibration-like excitations, but that of $Ba^{142}$ supports the suggestion of a transition to deformation effects as the neutron number approaches $N = 88$.

## I. INTRODUCTION

Recent advances in the study of short-lived activities have made available a large number of short-lived radionuclides free from contaminating activities. Many of the transitional nuclei with neutron numbers in the region $84 \leq N \leq 90$ are now available using "on-line" techniques for production and investigation. The on-line isotope separator system TRISTAN at the Ames Laboratory research reactor[1,2] is currently being used to make available for study the short-lived gaseous fission products

and their daughters; initial investigations have been directed toward the determination of half-lives and delayed neutron emission properties for these nuclei.[3,4] In this work, the $A = 142$ nuclei in the isobaric decay chain, starting with the decay of $Xe^{142}$ produced in thermal-neutron fission of $U^{235}$, were studied with large volume Ge(Li) detectors, both in singles measurements and in coincidence measurements.

The $\gamma$-ray transitions in the four nuclei reported here, $Cs^{142}$, $Ba^{142}$, $La^{142}$, and $Ce^{142}$, have been poorly studied in the past, mainly because of the inability to obtain pure samples of reasonable activity for the parent nuclei. An incomplete $\gamma$-ray list for all four nuclei has been reported by Alvager *et al.*,[5] and $\gamma$ rays from transitions in $La^{142}$ have been reported by Fritze and Kennett[6] and by Schuman, Turk, and Heath.[7] No investigator attempted to construct a decay scheme. The decay of $La^{142}$ has been more extensively studied recently,[8-10] and a partial level scheme for $Ce^{142}$ exists from these studies.[11,12]

The transitional nuclei with neutron numbers greater than $N = 82$ are of interest, since they progress from the vibration-like structure of the near-spherical nuclei to the rotational behavior of the deformed region of the rare-earth nuclei. Just what the relationship is between the structures on either side of this transitional region is not known. Several attempts have been made to describe the behavior of similar transitional nuclei.[13-15] The numerical technique of Kumar and Baranger[16-20] has met with some success in the heavy transition region which includes the even-even tungsten, osmium, and platinum nuclei.[21,22] Other theoretical approaches may be attractive in describing these transitional nuclei; the variable-moment-of-inertia model[23] may have some valid application in these nuclei, and there exist other recent attempts at simplified microscopic calculations which may prove to be useful.[24,25]

In addition to the classification of transition energies and intensities and the development of level schemes, an effort is made in the present study to identify the underlying behavior of the levels found; i.e., to determine whether vibrational and/or rotational features are easily identified.

## II. PROCEDURE

The short-lived $Xe^{142}$ parent activity for these studies was produced from fissions induced in 650 mg of $U^{235}$ (in the form of uranyl stearate) placed in a neutron beam of approximately $3 \times 10^9 n_{th}/cm^2$ sec; this sample has excellent emanation properties for the inert gases.[26] The xenon gas was transported from the uranium sample through a 2-m transport line (i.d. 1.27 cm) into the ion source of the isotope separator with the aid of a sweep gas (98% He, 1% Kr, 1% Xe); the average transit time to the ion source has been measured to be less than 1 sec. The entire fission-product generation assembly was operated at a 60-kV acceleration potential of the isotope separator, thus overcoming the problems encountered in the use of a fissioning sample placed at ground potential within the reactor.[2]

Mass separation of the gaseous fission products was accomplished by use of a Scandinavian electromagnetic isotope separator. Ions of the particular mass of interest, in this work 142, were directed through a slit in the focal plane of the separator and collected on a metallic surface at the secondary focus of a beam-switching magnet; the adjacent mass contamination was less than one part in $10^4$.

The decay of $La^{142}$ has a half-life of 92.5 min, which allows standard radiochemical techniques to be used to separate this activity from its precursor activities. The ion beam of the separator was deposited on a thin copper foil for approximately three half-lives of $La^{142}$, removed from the vacuum system of the separator, and set aside for 30 min to allow the 10.7-min $Ba^{142}$ decay to $La^{142}$ to be completed. The lanthanum was then separated from the remaining activity in the form of $La(OH)_3$ and placed before the appropriate detector to form a small source with negligible self-absorption of the $\gamma$ radiation.

The half-lives of $Xe^{142}$ and $Cs^{142}$ are quite similar, with values of 1.24 and 1.67 sec, respectively. Activities with half-lives this short must be studied "on line" with the aid of a moving-tape collector.[27] The xenon decay activity is enhanced by collecting the ions on an aluminum-Mylar tape while observing the $\gamma$ radiations coming from the region of deposit through a collimator. The residual daughter activities are carried behind the collimator shielding by moving the tape at a continuous rate. The cesium daughter activity can also be observed at the point of ion beam collection and can be enhanced by operating the tape collector in a discontinuous mode. In this mode, the ion beam is collected for a preset time and deflected from the tape during a time interval selected to allow preferential decay of the parent xenon activity, then the detector system switched on to count the residual (enhanced) cesium activity. At the end of the counting period the tape can be moved to carry any remaining activity to a shielded location and to bring a fresh portion of collection tape into position for a repetition of the collection, deflection, and measurement cycle. For the specific enhancement of $Cs^{142}$ activity, optimization of the

collection, delay, and analyze times by computer analysis resulted in values of: collection time of 5 sec, delay time of 5 sec, and analyze time of 6 sec. Although this use of the moving-tape collector yielded enhancement of the parent xenon or daughter cesium activity, there was significant contribution in each spectrum from the opposing decay. The separation and identification of the individual transitions was obtained by comparing the two spectra for relative enhancements, which worked well for the more intense peaks (see Fig. 1).

Since the 10.7-min $Ba^{142}$ activity is difficult to separate radiochemically within the time limitations imposed by the half-life, this activity was isolated by use of the moving-tape collector in another mode. The beam was collected for about three half-lives of the $Ba^{142}$ activity, then the deposit was transported within 20 sec to another detector station shielded from the collection port and was analyzed for the three half-life periods required to collect a new sample at the ion beam collection port. The cycle was repeated until adequate statistics were accumulated in the $\gamma$-ray spectrum. With this technique, a contribution was present from the $La^{142}$ decay, but was easily identified from previous studies of the decay of radiochemically separated $La^{142}$.

## III. DATA ACCUMULATION AND ANALYSES

The singles spectra from the four activities were measured using standard high-resolution detector electronics and an 8192-channel analog-to-digital converter (ADC). Three Ge(Li) detectors were used in the measurements: a 6-$cm^3$ planar detector which has excellent resolution at low energies, and two 30-$cm^3$ five-sided detectors (with a system resolution of 2.8 keV at 1.33 MeV) which were used primarily for the region above 500 keV and for coincidence measurements.

Coincidence data were collected in two experiments, each lasting four days. The $Xe^{142}$ and $Cs^{142}$ activities were studied together using the tape collector in a continuous on-line mode, while the

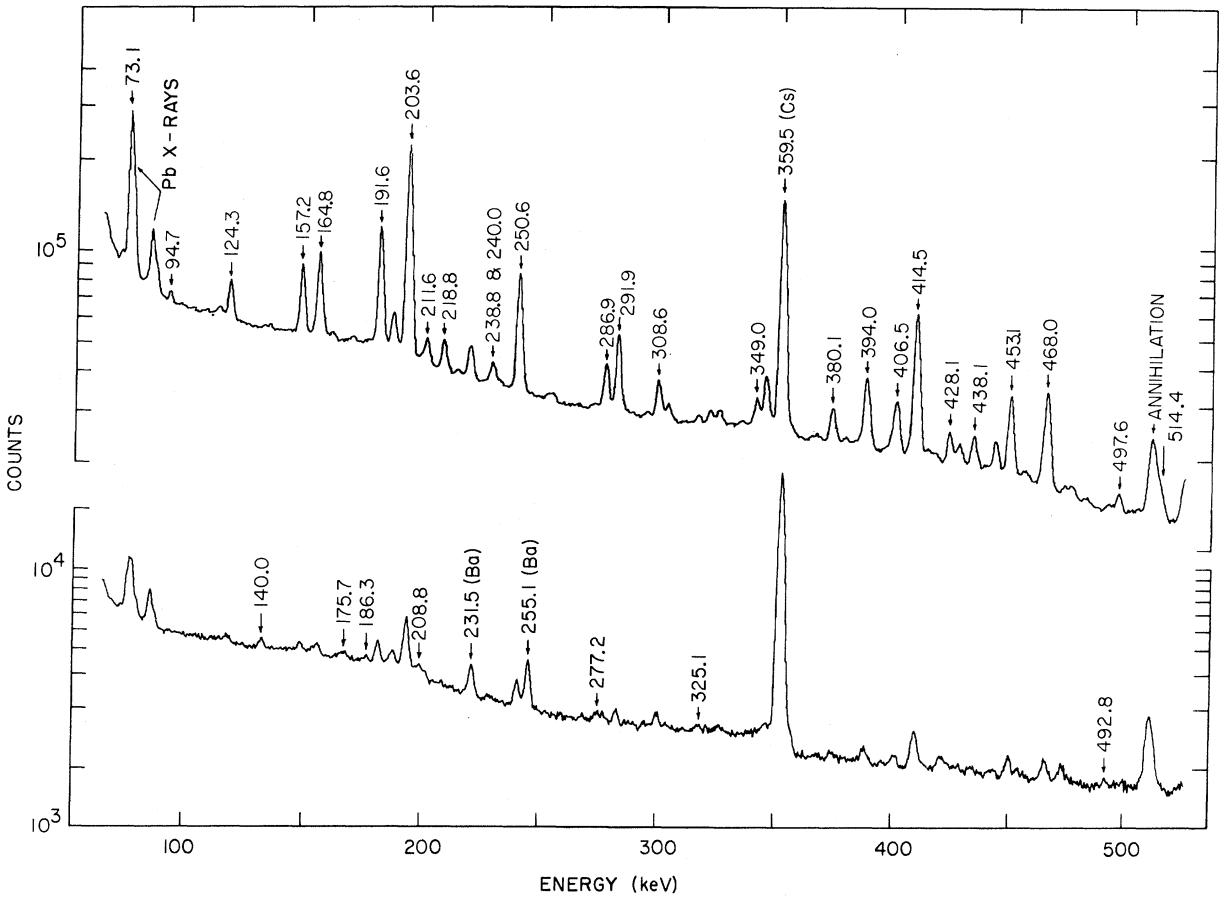


FIG. 1. Low-energy (70–530-keV) singles spectra for $Xe^{142}$ decay enhanced (upper curve) and $Cs^{142}$ decay enhanced (lower curve).

$Ba^{142}$ and $La^{142}$ activities were observed off line without chemical separation. The 30-$cm^3$ detectors were used in both experiments with coincidence timing determined from the use of commercial constant-fraction pick-off units. The outputs of the timing units were used to drive a time-to-amplitude converter which provided the coincidence gate to the ADC's after amplitude selection of the converter output by a single-channel analyzer. The resolving time of the system was set to be about 100 nsec. The linear signals were processed in two 4096-channel ADC's, and digital addresses for each event were recorded pairwise in a buffer memory and transferred to magnetic tape. With this system, a 4096-by-4096 matrix was recorded in the coincidence experiments. Playback of the magnetic tape through digital restriction gates into a large-memory multichannel analyzer enabled the sorting of coincidence events from the matrix into coincidence spectra selected by the windows placed about photopeaks in the spectrum of one detector. To correct for Compton-background coincidence events, an additional window of the same width was placed adjacent to each photopeak window. The coincidence experiment results were used mainly in a qualitative manner, with a few quantitative intensity determinations made in coincidence spectra for the case of the long-lived $La^{142}$ decay.

The unknown singles spectra, together with spectra obtained for standard calibration sources, were analyzed using standard computer peak-fitting routines to give the centroid and area of each photopeak. Corrections were made for the nonlinearity of the detector system, $\gamma$-ray attenuations, and detector efficiency; and energies and intensities of the transitions with associated standard errors were determined. The relatively weak sources available and detector geometries used for these experiments did not show any photopeaks corresponding to accidental summing in the detectors. Escape peaks were identified by energy differences from full-energy peaks, peak widths, and relative intensities.

## IV. DECAY SCHEMES

### A. Decay of 1.24-sec $Xe^{142}$

A portion of the low-energy singles spectra of the enhanced xenon decay (upper curve) and enhanced cesium decay (lower curve) is shown in Fig. 1. Comparison of the two spectra shows that many photopeaks can be assigned unambiguously to one of the two decays. The highest-energy $\gamma$ ray apparent in the xenon-enhanced studies is at 2078 keV. Since the xenon enhancement is quite marked and all higher-energy transitions are weak in either spectrum, and since there is a considerable difference between the decay energies expected for the decays of $Xe^{142}$ and $Cs^{142}$ (4.34 and 7.24 MeV, respectively[28]), it has been assumed that the $\gamma$ rays of higher energy belong to the cesium decay. A summary of $\gamma$-ray transitions in $Cs^{142}$ is presented in Table I. Many of the weak transitions included are only tentatively attributed to the xenon decay. The observed coincidences between the more intense transitions are listed in Table II.

The proposed level scheme for $Cs^{142}$ is shown in Figs. 2 and 3. The low-lying levels in $Cs^{142}$ are shown in Fig. 2, while the higher-lying levels appear in Fig. 3. The existence of the level at 12.2 keV is inferred from the observation that several pairs of transitions differ in energy by this amount, and from $\gamma$-ray cascades deduced from the coincidence data. The levels at 39.0 and 85.4 keV were placed from the consideration of the coincidence relations between the 73.1-, 124.3-, 157.2-, 164.8-, 203.6-, 218.8-, 414.5-, 538.1-, and 571.7-keV $\gamma$ rays. These coincidence relations also require the presence of two 39.0-keV transitions in order to account for the cascades indicated. A 33.0-keV transition, which is difficult to observe since it coincides in energy with the $K_\beta$ Cs x ray, is placed between the 242.5- and 209.5-keV levels to account for possible coincidences of the 124.3-keV transition with the 414.5-keV transition and the 197.2-keV transition with the 414.5-keV transition.

Additionally, a second 203.6-keV transition is placed in direct cascade with the 414.5-keV $\gamma$ ray to account for the very strong coincidence observed; the 191.6-keV transition is not seen in as strong a coincidence with the 414.5-keV transition as would be expected for only a single 203.6-keV transition to the ground state. The 191.6-keV and lower 203.6-keV transitions are placed in parallel to explain the several coincidence relations involving both of these peaks. An estimate of the intensities of the two 203.6-keV transitions is based on the 414.5-keV gated spectrum.

On the basis of the $\gamma$-ray placements, most of the $\beta$-decay strength to excited states appears as branching to the 656.8-keV level and, depending on the characters of the low-energy transitions and hence the magnitudes of the internal-conversion coefficients, possibly to the levels at 12.2, 39.0, 70.4, and 85.4 keV. No information exists on the ground-state $\beta$ branching. Future studies should include attempts to directly observe the intensities of the $\gamma$-ray transitions between these low-lying levels, and an attempt to determine their multipolarities. The calculation of comparative half-lives will depend upon success in these future studies.

TABLE I. $\gamma$-ray transitions in $Cs^{142}$.

| Energy (keV) | Relative intensity [a] | Energy (keV) | Relative intensity [a] | Energy (keV) | Relative intensity [a] | Energy (keV) | Relative intensity [a] |
|---|---|---|---|---|---|---|---|
| 12.2 ±0.1 | b | 329.8 ±0.2 | 17±4 | 693.5 ±0.3 | 48±10 | 1258.17±0.10 | 99±19 |
| 33.0 ±c | c | 333.7 ±0.2 | 21±5 | 709.4 ±0.2 | 16±4 | 1266 ±1 | 6±2 |
| 39.0 ±0.2 | d,e | 337.9 ±0.4 | 7±3 | 712.3 ±0.6 | 11±3 | 1300.24±0.08 | 397±58 |
| 46.4 ±0.2 | d | 342.2 ±0.4 | 9±3 | 718.2 ±0.3 | 10±3 [e] | 1303.6 ±0.5 | 41±8 |
| 57.6 ±0.3 | d,e | 349.0 ±0.2 | 58±12 | 724.8 ±0.8 | 10±3 | 1312.34±0.09 | 286±44 |
| 59.7 ±0.3 | d | 352.84±0.05 | 108±21 | 727.2 ±0.6 | 14±4 | 1338.3 ±0.5 | 29±6 |
| 68.3 ±0.2 | d | 373.2 ±0.4 | 10±3 | 734.6 ±0.3 | 41±9 | 1362.4 ±0.9 | 15±4 |
| 70.4 ±0.2 | d | 380.13±0.09 | 63±13 | 737.1 ±0.2 | 157±30 | 1377.4 ±0.4 | 14±4 |
| 73.14±0.11 | 454±130 [f] | 394.03±0.05 | 146±28 | 740.5 ±0.2 | 28±6 | 1384.5 ±0.3 | 14±4 |
| 94.65±0.10 | 15±4 | 404.7 ±0.3 | 28±6 | 744.6 ±0.2 | 22±5 | 1395.0 ±0.3 | 18±5 |
| 100.5 ±0.2 | 6±2 [e] | 406.5 ±0.2 | 105±20 | 761.1 ±0.3 | 20±5 | 1410.50±0.15 | 88±17 |
| 105.6 ±0.3 | 5±2 | 411.6 ±0.4 | 13±4 | 765.5 ±0.2 | 41±9 | 1432.3 ±0.9 | 15±4 |
| 113.0 ±0.5 | 2±1 | 414.45±0.15 | 430±69 | 775.9 ±0.4 | 33±7 | 1455.8 ±0.5 | 12±4 |
| 118.3 ±0.2 | 7±2 [e] | 418.7 ±0.3 | 19±5 | 792.0 ±0.4 | 12±3 | 1472.8 ±0.3 | 20±5 |
| 120.2 ±0.3 | 5±2 | 421.7 ±0.5 | 11±3 | 801.1 ±0.2 | 68±14 | 1486.5 ±0.8 | 17±5 |
| 124.31±0.04 | 62±15 | 428.11±0.10 | 54±11 | 806.7 ±0.2 | 69±14 | 1511.4 ±0.4 | 15±4 |
| 142.5 ±0.3 | 6±2 | 432.07±0.15 | 38±8 | 815.4 ±0.3 | 37±8 | 1519.7 ±0.7 | 9±3 |
| 157.18±0.02 | 127±27 | 438.13±0.10 | 57±11 | 823.6 ±0.6 | 16±4 | 1542.3 ±0.4 | 11±3 |
| 162.5 ±0.5 | 4±2 | 442.8 ±0.4 | 13±3 | 830.5 ±0.5 | 19±5 | 1595.1 ±0.6 | 16±4 |
| 164.81±0.02 | 163±31 | 447.0 ±0.2 | 51±11 | 863.9 ±0.5 | 22±5 | 1602.4 ±0.2 | 23±5 |
| 167.0 ±0.2 | 11±3 | 453.05±0.04 | 182±33 | 891.5 ±0.3 | 115±21 | 1607.0 ±0.2 | 46±10 |
| 170.6 ±0.2 | 10±3 | 467.98±0.10 | 217±38 [e] | 900.8 ±0.2 | 13±4 | 1616.8 ±0.5 | 7±2 |
| 180.1 ±0.3 | 6±2 | 497.6 ±0.3 | 20±5 | 917.9 ±0.3 | 33±7 | 1625.2 ±0.4 | 11±3 |
| 191.56±0.02 | 283±51 | 514.4 ±0.3 | 40±9 | 930.8 ±0.2 | 21±5 | 1633.1 ±0.2 | 21±5 |
| 197.19±0.07 | 57±12 | 524.28±0.12 | 54±11 | 943.4 ±0.5 | 29±6 | 1640.0 ±0.8 | 5±2 |
| 203.64±0.05 | 215±59 [e] | 538.12±0.03 | 752±100 | 957.3 ±0.2 | 66±13 | 1663.6 ±0.5 | 12±3 |
| | (to g.s.) | 547.44±0.12 | 63±12 | 982.4 ±0.4 | 20±5 | 1671.9 ±0.5 | 17±4 |
| | 503±125 | 557.6 ±0.2 | 51±11 | 991.5 ±0.2 | 79±14 | 1711.0 ±0.2 | 25±6 |
| | (to 39 keV) | 562.3 ±0.5 | 20±5 | 997.0 ±0.3 | 39±8 | 1718.9 ±0.3 | 19±5 |
| 211.56±0.06 | 40±8 | 571.66±0.02 | 1000±103 | 1019.6 ±0.5 | 30±6 | 1744.8 ±0.9 | 14±4 |
| 218.84±0.05 | 47±8 | 578.3 ±0.3 | 28±6 | 1041.3 ±0.8 | 15±5 | 1756.9 ±0.3 | 15±4 |
| 224.2 ±0.5 | 5±2 | 582.4 ±0.2 | 52±11 | 1049.5 ±0.9 | 12±4 | 1774.8 ±0.4 | 11±3 |
| 230.22±0.05 | 47±8 | 586.7 ±0.2 | 36±7 | 1056.0 ±0.7 | 5±2 | 1781.0 ±0.3 | 12±3 |
| 238.8 ±0.5 [g] | 17±4 | 598.2 ±0.2 | 52±11 | 1068.2 ±0.4 | 44±8 | 1790.7 ±0.5 | 12±3 |
| 240.0 ±0.4 [g] | 17±4 | 605.47±0.06 | 218±32 | 1089.4 ±0.6 | 15±4 | 1805.2 ±0.7 | 10±3 |
| 242.5 ±0.4 | 7±3 | 617.82±0.04 | 763±99 | 1108.3 ±0.5 | 22±5 [e] | 1832.4 ±0.4 | 37±8 |
| 250.59±0.02 | 260±44 | 627.4 ±0.6 | 6±2 | 1156.9 ±0.2 | 67±11 | 1837.0 ±0.3 | 36±8 |
| 262.6 ±0.4 | 5±2 | 642.5 ±0.3 | 96±18 | 1164.7 ±0.4 | 27±6 | 1844.3 ±0.2 | 28±6 |
| 265.1 ±0.3 | 10 ±3 | 644.55±0.04 | 628±81 | 1183.7 ±0.5 | 22±8 | 1862.2 ±0.2 | 21±6 |
| 286.89±0.04 | 78±16 | 656.83±0.08 | 825±91 | 1187.3 ±0.2 | 67±12 | 1875.5 ±0.3 | 30±7 |
| 291.88±0.03 | 152±29 | 662.0 ±0.5 | 28±6 | 1194.6 ±0.2 | 70±15 | 1902.1 ±0.2 | 65±14 |
| 303.8 ±0.4 | 9±3 | 664.4 ±0.2 | 193±31 | 1219.18±0.09 | 82±16 | 1972.2 ±0.5 | 18±5 |
| 308.59±0.05 | 71±15 | 669.0 ±0.4 | 20±4 | 1227.12±0.07 | 242±40 | 1996.3 ±0.4 | 18±5 |
| 312.6 ±0.2 | 27±6 | 672.0 ±0.2 | 69±19 | 1232.9 ±0.2 | 42±9 | 2078.5 ±0.4 | 22±5 |

[a] Measured relative to the 571.7-keV transition.
[b] Transition below the detector threshold; intensity unknown.
[c] If this transition exists, it coincides with the Cs x rays, making accurate measurement difficult.
[d] Detector efficiency not known for this energy.
[e] Used in more than one place in level scheme.
[f] Estimated; Pb x rays interfere with measurements.
[g] Possibly a singlet at 239.4 keV.

### B. Decay of 1.67-sec $Cs^{142}$

The most elusive decay of the four nuclei which were investigated is that of $Cs^{142}$ to $Ba^{142}$. The measured $\gamma$-ray energies are listed in Table III together with intensities. Errors quoted for both quantities are larger in most cases than those quoted for the other isobars because of the lack of adequate statistics for satisfactory computer fits to the data. Coincidence relations for transitions in $Ba^{142}$ are listed in Table IV.

There was great difficulty in the construction of

TABLE II. $\gamma$-ray coincidence in $Cs^{142}$.

| Gating transition (keV) | Coincidence transitions (keV) |
|---|---|
| 73.1 | 124.3, 157.2, 218.8, 414.5, 538.1, 571.7 |
| 94.7 | 124.3, 197.2 |
| 124.3 | 73.1, 94.7, 414.5 (?), 547.4 |
| 157.2 | 73.1, 414.5, 538.1 |
| 164.8 | 414.5, 453.1 |
| 191.6 | 406.5 (?), 414.5, 453.1 |
| 197.2 | 94.7, 414.5 (?), 547.4 |
| 203.6 | 394.0, 406.5 (?), 414.5, 453.1, 514.4, 538.1 |
| 211.6 | 406.5, 1108.3 (?) |
| 218.8 | 73.1, 352.8 |
| 230.2 | 414.5, 538.1 |
| 250.6 | 349.0, 406.5 |
| 286.9 | 352.8 |
| 291.9 | 352.8, 891.5 |
| 349.0 | 250.6 |
| 394.0 | 191.6, 203.6 |
| 406.5 | 250.6 |
| 414.5 | 73.1, 157.2, 164.8, 191.6, 203.6, 230.2, 538.1 |
| 514.4 | 203.6 |
| 524.3 | 250.6 |
| 538.1 | 157.2, 191.6, 203.6, 230.2, 250.6, 352.8, 414.5, 453.1, 571.7, 617.8, 644.6, 656.8 |
| 571.7 | 73.1, 538.1 |
| 617.8 | 538.1 |
| 644.6 | 538.1 |
| 656.8 | 538.1 |

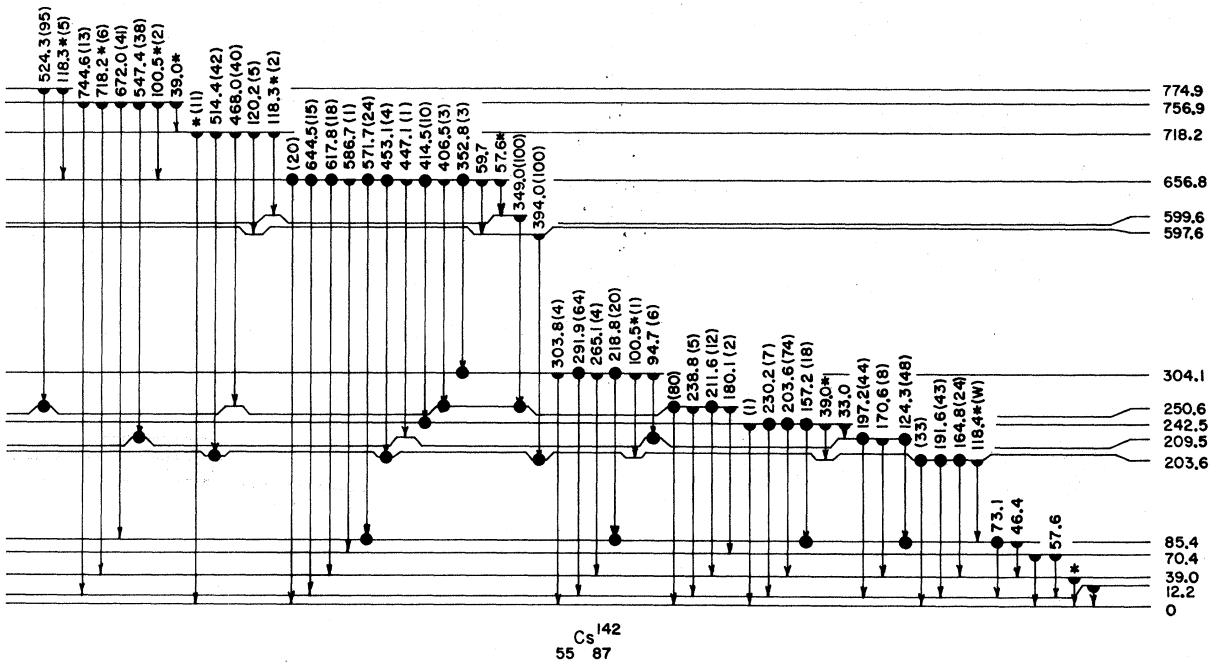


FIG. 2. Low-energy level scheme for $Cs^{142}$. * indicates $\gamma$ ray was used more than once, ● indicates coincidence.

a comprehensive decay scheme; the resulting partial level scheme is shown in Fig. 4, in which levels are indicated only if supported by coincidence data or unique energy sums for cascade transitions. Despite the incompleteness of this level scheme, in which the multitude of high-energy transitions has been ignored, it still accommodates about 60% of the $\gamma$-ray intensity assigned to this decay. The information presented here for the decay of $Cs^{142}$ is clearly preliminary, but the level scheme does offer some interesting conclusions, to be discussed later.

### C. Decay of 10.7-min $Ba^{142}$

55 $\gamma$-ray transitions have been identified in the deexcitation of the levels in $La^{142}$. The highest-energy transition is at 1379.9 keV. The observed $\gamma$-ray energies and intensities are listed in Table V, and coincidence relations are summarized in Table VI. All but four of the listed transitions have been placed into the level scheme for $La^{142}$ (Fig. 5). A $\gamma$-ray multiplet was observed at approximately 62 keV, but has not been considered in the construction of the decay scheme.

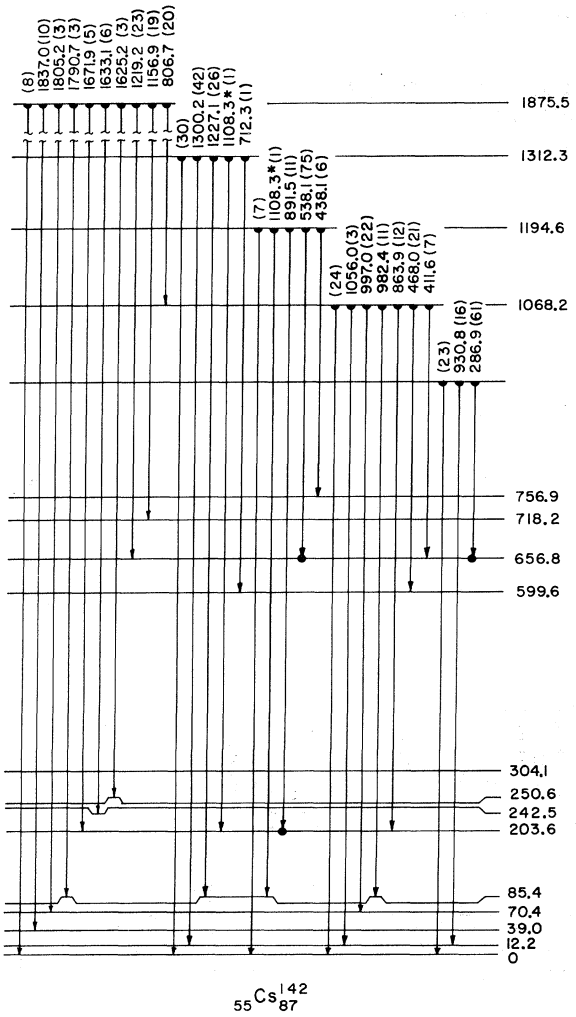


FIG. 3. High-energy level scheme for $Cs^{142}$. Symbols as in Fig. 2.

The strong transition at 77.6 keV is placed as the ground-state transition from the first excited state; the proximity of this $\gamma$ ray to the lead x rays in the spectrum is a factor in the intensity and energy uncertainties for this transition, which are larger than for the more well-defined $\gamma$ rays. The total $\gamma$-ray intensity feeding the 77.6-keV level exceeds that depopulating the state, indicating the presence of appreciable internal conversion for this transition. If no $\beta$ branching to this level is considered, the minimum total internal-conversion coefficient must be 1.7, which is close to that for a pure $M1$ transition at this energy. The value of 2.26 for a pure $M1$ transition[29] was used in the calculation of a 6% $\beta$ branching to the 77.6-keV level. A similar situation is observed in the decay of $Ba^{140}$, for which the 30-keV transition in $La^{140}$ has a measured multipolarity of pure $M1$.[30]

For the purpose of calculating $\beta$ branching ratios and comparative half-lives, the decay energy is assumed to be 1.88 MeV, according to the mass tables of Garvey *et al.*,[28] and the ground-state $\beta$ branching is assumed to be negligible (a ground-state branching of 20% would give a ground-state log*ft* value of 6.1 and would increase the other log*ft* values by only 0.1). The results of the $\beta$-branching calculations appear in Table VII.

### D. Decay of 92.4-min $La^{142}$

The $\gamma$-ray spectrum for this decay is characterized by intense peaks at 641.2, 894.9, 1901.3, 2187.2, 2397.7, and 2542.7 keV. The observed photopeak energies and intensities are shown in Table VIII, while coincidence relations appear in Table IX. 90 $\gamma$-ray transitions have been placed in a decay scheme of 25 excited levels, shown in Figs. 6 and 7. The low- and high-energy states are shown in Figs. 6 and 7, respectively. The important low-energy levels are located at 641.2, 1219.3, 1536.1, 1652.6, 2004.2, 2397.7, and 2542.7 keV; these states are firmly established both by energy sums and coincidence relations.

$\beta$-branching percentages and comparative half-lives are summarized in Table X, and result from the assumption of a 13% ground-state $\beta$ branch.[9] Two intense branches to the 2397.7- and 2542.7-keV levels, combined with the ground-state branch, comprise the major part of the $\beta$-decay strength. A complete $\beta$-decay scheme is shown in Fig. 8, where the decay energy is assumed to be 4.50 MeV,

TABLE III. $\gamma$-ray transitions in $Ba^{142}$.

| Energy (keV) | Relative intensity [a] | Energy (keV) | Relative intensity [a] | Energy (keV) | Relative intensity [a] | Energy (keV) | Relative intensity [a] |
|---|---|---|---|---|---|---|---|
| 140.0 ±0.6 | 7±4 | 1898.81±0.09 | 50±9 | 2784.6 ±0.3 | 10±4 | 4028.1 ±0.4 [c] | 7±3 |
| 175.7 ±0.7 | 6±3 | 1915.6 ±0.2 | 12±4 | 2795.7 ±0.5 | 5±2 | 4036.6 ±0.4 [c] | 7±3 |
| 186.3 ±0.3 | 5±3 | 1935.3 ±0.15 | 20±5 | 2840.2 ±0.3 | 9±3 | 4086.5 ±0.5 | 6±3 |
| 208.8 ±0.4 | 5±3 | 1957.0 ±0.5 | 16±4 | 2856.1 ±0.5 | 5±2 | 4096.1 ±0.3 | 10±3 |
| 277.2 ±0.8 | 5±3 | 1960.9 ±0.5 | 8±3 | 2882.50±0.11 | 26±6 | 4145.0 ±0.7 | 4±2 |
| 281.8 ±0.6 | 5±3 | 1982.1 ±0.1 | 63±12 | 2924.10±0.10 | 38±7 | 4178.6 ±0.5 | 5±2 |
| 325.1 ±0.5 | 6±3 | 2006.6 ±0.8 | 4±2 | 2939.1 ±0.4 | 9±3 | 4198.1 ±0.5 | 5±2 |
| 359.52±0.02 | 1000±94 | 2050.2 ±0.6 | 4±2 | 2987.5 ±0.6 | 5±2 | 4205.4 ±0.7 | 4±2 |
| 401.6 ±0.5 | 7±3 | 2057.2 ±0.5 | 5±2 | 2992.6 ±0.5 | 6±3 | 4218.5 ±1.0 | 2±1 |
| 459.3 ±0.6 | 10±4 | 2152.0 ±0.5 | 5±2 | 3079.7 ±0.7 | 5±2 | 4237.1 ±0.2 | 17±4 |
| 475.0 ±0.3 | 12±4 | 2165.4 ±0.5 | 5±2 | 3144.4 ±0.2 | 14±4 | 4249.4 ±0.4 | 6±3 |
| 492.8 ±0.6 | 2±1 | 2186.1 ±0.8 | 4±2 | 3167.3 ±0.4 | 9±3 | 4276.5 ±0.3 | 6±3 |
| 608.4 ±0.2 | 3±1 | 2191.7 ±0.7 | 4±2 | 3182.3 ±0.6 | 6±3 | 4362.5 ±0.8 | 3±2 |
| 635.4 ±0.6 | 2±1 | 2246.5 ±0.1 [c] | 32±7 | 3262.0 ±0.4 | 11±4 | 4369.3 ±0.2 | 22±5 |
| 841.0 ±0.5 | 2±1 | 2254.1 ±0.2 | 22±6 | 3282.9 ±0.2 | 41±8 | 4388.9 ±0.6 | 5±2 |
| 857.3 ±0.5 | 14±5 | 2286.2 ±0.9 | 4±2 | 3310.2 ±0.8 | 4±2 | 4396.1 ±0.8 | 3±1 |
| 915.4 ±0.7 | 11±4 | 2300.0 ±0.4 | 7±3 | 3368.9 ±0.5 | 7±3 | 4418.0 ±0.2 | 21±5 |
| 932.9 ±0.2 | 27±6 | 2334.6 ±0.4 | 7±3 | 3402.9 ±0.9 | 3±2 | 4494.2 ±0.4 | 6±3 |
| 966.92±0.10 | 365±70 | 2341.4 ±0.2 | 12±4 | 3426.1 ±0.2 | 21±5 | 4538.6 ±0.7 | 3±1 |
| 986.2 ±0.4 | 17±4 | 2351.2 ±0.3 | 11±4 | 3573.03±0.09 | 49±10 | 4549.5 ±0.4 | 4±2 |
| 1015.3 ±0.5 | 11±3 | 2393.4 ±0.5 | 7±3 | 3662.5 ±0.4 | 10±3 | 4564.8 ±0.4 | 5±2 |
| 1064.2 ±0.4 | 32±6 | 2397.6 ±0.2 | 18±5 | 3667.9 ±0.9 [c] | 2±1 | 4577.2 ±0.5 | 4±2 |
| 1100.6 ±0.3 | 21±5 | 2411.7 ±0.4 | 9±3 | 3786.6 ±0.2 | 16±4 | 4609.5 ±0.4 | 5±2 |
| 1118.2 ±0.6 | 10±4 | 2444.4 ±0.7 | 3±2 | 3798.2 ±0.2 | 19±4 | 4647.2 ±0.4 | 7±3 |
| 1137.5 ±0.5 | 9±4 | 2455.2 ±0.5 | 5±2 | 3835.0 ±0.2 | 22±5 | 4668.2 ±1.1 | 2±1 |
| 1175.88±0.08 | 119±24 | 2499.8 ±0.6 | 4±2 | 3852.7 ±0.7 | 6±3 | 4691.9 ±1.3 | 2±1 |
| 1192.6 ±0.4 | 16±5 | 2508.3 ±0.4 | 7±3 | 3870.5 ±0.2 [b] | 13±4 | 4697.6 ±1.0 | 3±1 |
| 1243.5 ±0.1 | 17±6 | 2522.6 ±0.2 | 19±5 | 3876.8 ±0.8 | 7±3 | 4730.7 ±1.0 | 2±1 |
| 1279.88±0.07 | 73±13 | 2544.5 ±0.4 | 7±3 | 3881.7 ±1.3 | 4±2 | 4811.5 ±0.9 | 2±1 |
| 1326.48±0.02 | 362±56 | 2555.4 ±0.9 | 4±2 | 3897.3 ±0.4 | 8±3 | 4862.4 ±0.7 | 3±1 |
| 1333.1 ±0.2 | 50±11 | 2575.7 ±0.7 | 5±2 | 3931.7 ±0.2 | 22±5 | 4874.5 ±1.1 | 1±1 |
| 1349 ±1 | 3±1 | 2613.6 ±0.3 | 9±3 | 3938.7 ±0.6 | 5±2 | 4892.3 ±0.6 | 3±1 |
| 1422.96±0.05 | 80±17 | 2655.2 ±0.4 | 7±3 | 3953.7 ±1.0 | 3±2 | 4935.4 ±1.1 | 2±1 |
| 1559.7 ±0.1 | 32±10 | 2676.5 ±0.4 | 6±3 | 3982.4 ±0.5 [c] | 3±2 | 5112.5 ±0.8 | 2±1 |
| 1610.9 ±0.2 | 15±5 | 2720.0 ±0.8 | 5±2 | 4008.8 ±0.8 | 4±2 | 5393.6 ±0.7 | 1±1 |
| 1768.5 ±0.1 | 21±6 | 2725.3 ±0.2 | 32±7 | | | | |
| 1818.1 ±0.1 [b] | 18±5 | 2757.2 ±0.2 | 22±5 | | | | |

[a] Measured relative to the 359.5-keV transition.
[b] A double-escape peak is also found at this energy.
[c] A single-escape peak is also found at this energy.

again from the mass tables of Garvey *et al.*[28]

## V. DISCUSSION

The known decay schemes in this mass region display a preponderance of first-forbidden non-unique $\beta$ transitions. For the decays reported here, first-forbidden transitions are expected from consideration of the single-particle levels present near the Fermi surface for these nuclei. The most likely transition would be from an $f_{7/2}$ neutron to a $g_{7/2}$ proton. Other close-lying single-particle levels which may contribute $\beta$ strength are the $h_{9/2}$ neutron and $d_{5/2}$ proton levels. Any combination of these four single-particle states would give a first-forbidden $\beta$ decay. Accordingly, the comparative half-lives are expected to have a range of values for log$ft$ from about 6.0 to 10.5.[31]

Excited-state spins and parities may be estimated under the assumption that the $\gamma$-ray transitions observed are of $M1$, $E1$, or $E2$ character. Additionally, the systematics of levels in neighboring even-even nuclei should reveal tendencies for the low-lying energy levels which can be used to determine probable spin-parity assignments.

### A. Levels of $Cs^{142}$

Examination of similar odd-odd nuclei reveals that $M1$ transitions dominate between the low-lying states of these nuclei, and similar multipolarities can be expected for transitions between the low-

TABLE IV. $\gamma$-ray coincidences in $Ba^{142}$.

| Gating transition (keV) | Coincidence transitions (keV) |
|---|---|
| 359.5 | 475.0 (?), 966.9, 1064.4, 1100.6 (?), 1175.9, 1243.5 (?), 1279.9, 1333.1 (?), 1423.0, 1768.5, 1982.1 |
| 966.9 | 359.5 |
| 1064.2 | 359.5 |
| 1175.9 | 359.5 |
| 1279.9 | 359.5 |
| 1333.1 | 359.5 (?) |
| 1423.0 | 359.5 |
| 1982.1 | 359.5 |

TABLE V. $\gamma$-ray transitions in $La^{142}$.

| Energy (keV) | Relative intensity [a] | Energy (keV) | Relative intensity [a] |
|---|---|---|---|
| b | | 473.4 ±0.2 | 17±3 |
| 69.4 ±0.3 | 20 [c] | 488.3 ±0.5 | 6±4 |
| 76.8 ±0.6 | 50 [c,d] | 513.3 ±0.5 | 13±5 [f] |
| 77.6 ±0.1 | 540 [c,d] | 531.9 ±0.6 | 5±4 |
| 122.89±0.08 | 52±7 | 537.5 ±0.5 | 6±4 |
| 154.22±0.09 | 29±4 | 558.3 ±0.3 | 17±3 |
| 162.0 ±0.2 | 6±4 | 590.7 ±0.3 | 14±3 |
| 176.82±0.08 | 83±10 | 599.84±0.08 | 90±10 |
| 216.3 ±0.1 | 11±3 | 604.2 ±0.3 | 18±4 |
| 222.6 ±0.1 | 15±3 | 769.4 ±0.2 | 34±4 |
| 231.52±0.04 | 572±82 | 786.4 ±0.3 | 14±4 |
| 242.7 ±0.2 | 9±4 | 792.2 ±0.4 [g] | 12±4 |
| 255.12±0.04 | 1000±87 | 823.4 ±0.3 | 23±4 |
| 269.33±0.09 | 38±5 | 840.23±0.07 | 170±25 |
| 283.9 ±0.3 | 10±4 | 876.6 ±0.9 | 4±3 |
| 286.2 ±0.1 | 52±8 | 894.9 ±0.1 [h] | 615±64 |
| 309.02±0.05 | 127±17 | 948.75±0.06 | 500±70 |
| 334.8 ±0.1 | 70±10 | 1000.86±0.05 | 440±64 |
| 337.1 ±0.2 | 14±3 | 1032.8 ±0.3 | 27±4 |
| 346.7 ±0.5 | 8±4 | 1078.48±0.05 | 522±75 |
| 363.80±0.05 | 222±31 | 1093.62±0.06 | 124±17 |
| 379.1 ±0.1 | 26±4 | 1122.6 ±0.3 | 17±3 |
| 417.8 ±0.3 | 19±4 | 1126.54±0.08 | 86±12 |
| 425.03±0.06 | 275±40 | 1148.3 ±0.3 | 22±3 |
| 432.3 ±0.3 [e] | 55±8 | 1202.2 ±0.1 | 300±40 |
| 434.4 ±0.4 [e] | 17±3 | 1204.06±0.08 | 766±85 |
| 448.1 ±0.5 | 12±3 | 1283.4 ±0.5 | 9±4 |
| 457.3 ±0.2 | 22±4 | 1379.9 ±0.1 | 191±25 |

[a] Measured relative to the 255.1-keV transition.

[b] Several unresolved $\gamma$ rays near 62 keV.

[c] Estimated; detector efficiency is not well calibrated at these energies.

[d] Pb x rays are superimposed, making intensity measurements difficult.

[e] A 433.3-keV transition from $La^{142}$ decay is also present.

[f] Annihilation radiation interferes with intensity measurement; a 514.7-keV transition from $La^{142}$ decay is also present.

[g] A weak background line may be included.

[h] A $\gamma$ transition occurs at the same energy in the $La^{142}$ decay.

lying levels in $Cs^{142}$. The density of low-lying levels is similar also to that observed in $Cs^{140}$.[32] The ground state of this odd-odd cesium nucleus is expected to have odd parity and, as mentioned above, should be populated in $\beta$ decay by a first-forbidden transition. On the basis of systematics shown in neighboring odd-odd nuclei, the ground-state spin is likely to be $J=1$ or $J=2$.

Similarly, the expectation of $M1$ transitions between the first few excited states is consistent with the assumption that these states are likely to have odd parity, since the same neutron and proton subshells are probably involved in the $\beta$ decay to these low-lying levels. Any neutron excitation to the first even-parity orbit (the $i_{13/2}$ level) is too far above the Fermi level to be seen at low energies; however, even-parity states might be expected in the higher levels of the level scheme. Since the present work was confined to $\gamma$-ray spectroscopy, the inability to determine spins, parities, log$ft$ values, and internal-conversion coefficients for the levels in this nucleus prevents further interpretation of these levels.

### B. Levels of $Ba^{142}$

The spin-parity assignment for the ground state of this even-even nucleus is $0^+$, and for the first excited state at 359.5 keV it is $2^+$, because this state is the "so-called" one-phonon vibrational state. The second excited state at 1326.5 keV probably has $J^\pi = 2^+$, since strong $\gamma$ rays are observed to feed both the ground state and first excited state. The reduced transition probabilities between the second excited state and the ground state and the second $2^+$ to the first $2^+$ states have a ratio of

$$\frac{B(E2;\ 2_2^+ \rightarrow 0_0^+)}{B(E2;\ 2_2^+ \rightarrow 2_1^+)} = 0.21 \pm 0.07 .$$

This ratio is in agreement with that expected for a non-axially symmetric rotor assuming that the non-axial parameter can be determined from the energy ratios for the $2^+$ states.[33]

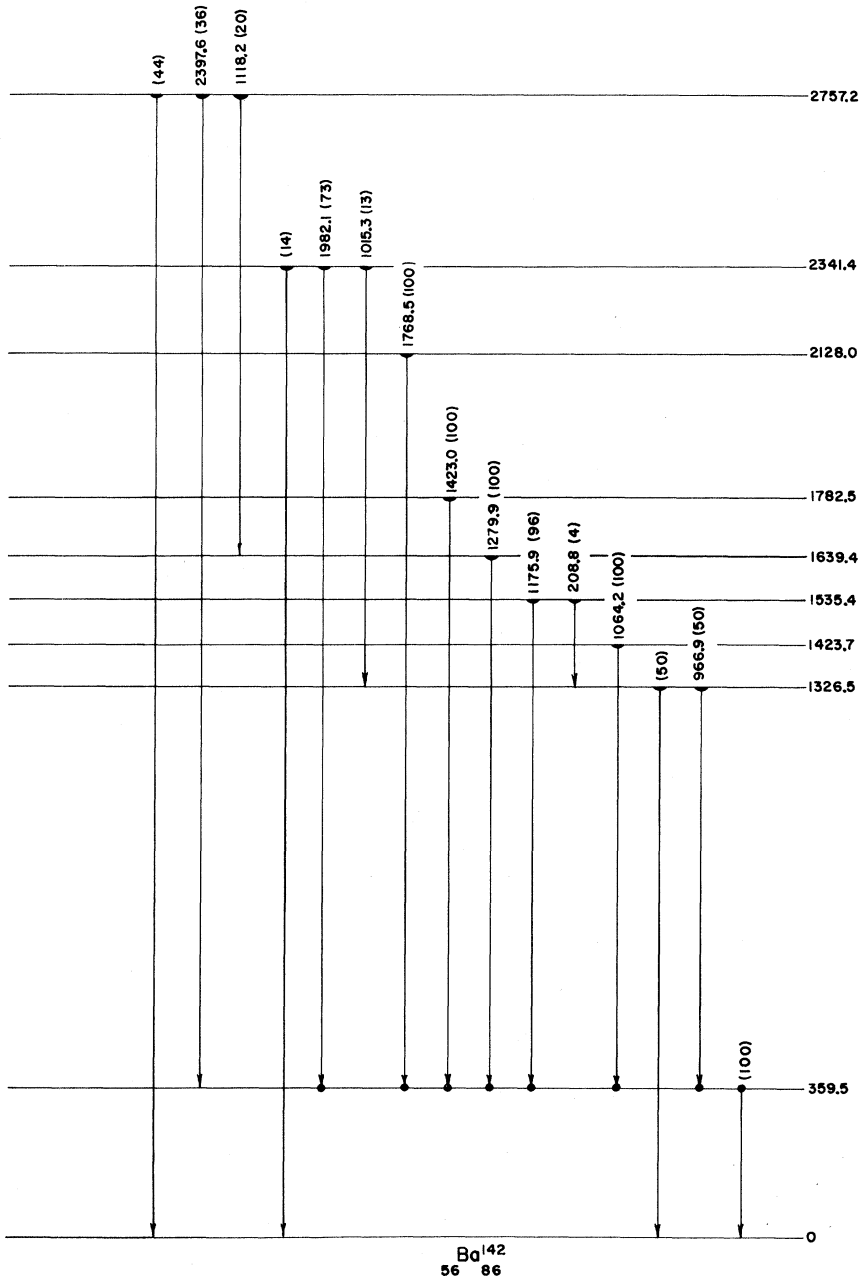


FIG. 4. Partial level scheme for $Ba^{142}$.

It is impossible to assign quantum numbers to the excited states above the 1326.5-keV level. Other nearby nuclides have states of $4^+$ and $3^-$ occurring fairly close to the second $2^+$ state, and similar states should be expected in this nuclide.

An interesting point is the apparent lack of a state intermediate to the 359.5- and 1356.5-keV levels. An illustration of systematic trends in the low-lying levels for $N = 86$ and $Z = 56$ nuclei is shown in Fig. 9. From the trends indicated, a level in the vicinity of 800 keV might be expected. There is weak experimental evidence in the present work for the existence of such a level; a very weak coincidence is observed between the 475.0- and 359.5-keV $\gamma$ rays which might be summed to a level at 834 keV. However, the decay intensity is very small and does not agree with that observed in $Ba^{140}$.[32] Population of this state, which might be expected to be the $4^+$ member of the two-phonon vibrational triplet, may be difficult if the spin of

TABLE VI. $\gamma$-ray coincidence in $La^{142}$.

| Gating transition (keV) | Coincidence transitions (keV) |
|---|---|
| 69.4 | 77.6, 216.3 |
| 77.6 | 122.9, 162.0, 222.6, 231.5, 283.9, 286.2, 599.8, 840.2, 894.9, 1100.9, 1093.6, 1126.5, 1379.9 |
| 122.9 | 77.6, 154.2 (?), 231.5, 309.0 |
| 154.2 | 122.9, 840.2 (?) |
| 162.0 | 69.4 |
| 176.8 | 255.1, 434.4 (?) |
| 216.3 | 77.6, 840.2 |
| 222.6 | 77.6 |
| 231.5 | 77.6, 122.9, 769.4, 894.9, 1148.3 (?) |
| 242.7 | 283.9, 599.8 |
| 255.1 | 176.8, 823.4, 948.8, 1202.2 |
| 269.3 | 334.8, 599.8 |
| 283.9 | 77.6 (?), 242.7 (?) |
| 286.2 | 77.6, 840.2, 1093.6 |
| 309.0 | 122.9, 894.9 |
| 334.8 | 269.3, 473.4 (?), 599.8, 1122.6 |
| 363.8 | 840.2, 1093.6 |
| 432.3 | 434.4 (?) |
| 434.4 | 122.9 (?), 176.8, 432.3 (?) |
| 599.8 | 242.7, 269.3, 283.9, 334.8, 448.1, 604.2 |
| 840.2 | 77.6, 154.2 (?), 216.3, 286.2, 363.8 |
| 894.9 | 77.6, 231.5, 309.0 |
| 948.8 | 255.1 |
| 1122.6 | 77.6 |
| 1126.5 | 77.6 |
| 1202.2 | 255.1 |
| 1379.9 | 77.6 |

the parent $Cs^{142}$ nucleus is low.

### C. Levels of $La^{142}$

The ground state of $La^{142}$ has been determined to have $J^\pi = 2^-$.[9] The first-excited-state-to-ground-state transition is probably $M1$ in character, which suggests a spin-parity of $1^-$ or $3^-$ for the 77.6-keV level. The estimated log$ft$ value of 6.6 (6% $\beta$ branching) would favor a $1^-$ assignment for the 77.6-keV level, since the $\beta$ transition appears to be first forbidden.

Spin-parity assignments for the next few levels cannot be made without an assignment for the 77.6-keV level. However, they are expected to have negative parity, and $M1$ and $E2$ transitions should occur between them. The log$ft$ values listed in Table VII are calculated from the $\gamma$-ray intensity balance for the various levels. Since the multipolarities of the transitions have not been experimentally determined, the internal-conversion corrections to these intensities cannot be calculated and the $\beta$ branches are subject to modification. A possible manifestation of this situation is seen in the very low log$ft$ values determined for the $\beta$ decays to some of the higher-lying states. An interesting possibility for the interpretation of these low log$ft$ values is that the states involved may exhibit some four-quasiparticle character involving $h_{9/2}$ and $h_{11/2}$ single-particle orbits.

### D. Levels of $Ce^{142}$

The important features of this decay are shown in Fig. 10. The first excited state is assumed to have $J^\pi = 2^+$ and would then be the one-phonon vibrational state. This level would be fed by a first-forbidden $\beta$ transition, which is consistent with the observed log$ft$ value of 9.0.

The state at 1219 keV is assigned $J^\pi = 4^+$ because no crossover transition to the ground state is found and the 578-keV stopover transition, even though it is not one of the stronger transitions observed, is in definite coincidence with the 641-keV $\gamma$ ray and with other transitions feeding this level. The level systematics for the neighboring $N = 84$ nuclei are shown in Fig. 11, in which a $4^+$ level occurs in both $Sm^{146}$ and $Nd^{144}$ and appears to follow a smooth contour with proton number. The corresponding level in $Ba^{140}$ agrees well with the indicated trend. The choice of the $4^+$ assignment is consistent with that expected from the vibrator

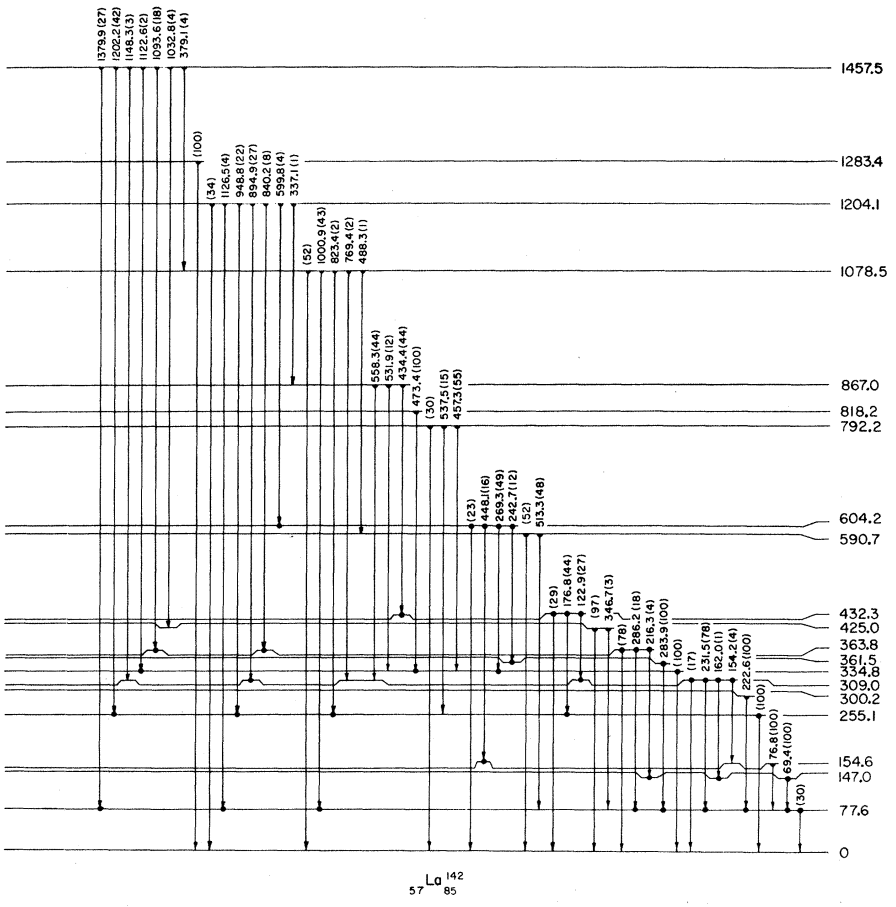


FIG. 5. Energy level scheme for $La^{142}$.

model; the $4^+$ member of the two-phonon triplet is at approximately twice the energy of the one-phonon singlet state.

A $2^+$ assignment is given to the 1536-keV level. The log*ft* value of 8.8 for the 3% $\beta$ branching to this level indicates a first-forbidden transition from the $2^-$ parent. The absence of a transition to the ground state supports the $2^+$ choice in that the $2_2^+ \rightarrow 0_0^+$ two-phonon transition is not allowed. This level is likely, then, to be the second member of the two-phonon triplet.

The level at 1653 keV is given an assignment of $3^-$, partly on the basis of the decay of this level to only the $2^+$ and $4^+$ levels, presumably by $E1$ transitions. This state is probably an octupole vibration state due to the very small (if not zero) $\beta$ feeding; the log*ft* of 9.1 rules out an allowed transition. A $\beta$ transition from the $2^-$ parent state to the $3^-$ excited state of the daughter is undoubtedly hindered if the two states involved have quite different character; the parent state is presumably a two-particle state (formed by a $f_{7/2}$ neutron and a $g_{7/2}$ proton), while the daughter state is collective in nature. Additional plausibility to the $3^-$ assignment is given by the trend seen in Fig. 11 for the $3^-$ levels in neighboring even-even nuclei with $N = 84$. Finally, assuming that this state does de-excite by $E1$ transitions, the reduced transition probabilities to the $2^+$ and $4^+$ states have a ratio of

$$\frac{B(E1;\ 3^- \rightarrow 2^+)}{B(E1;\ 3^- \rightarrow 4^+)} = 0.82 \pm 0.45,$$

which agrees well with the value of $0.82 \pm 0.50$ for the similar case in $Sm^{150}$.[34]

The 2004-keV level is assigned a spin-parity of $2^+$ because of $\gamma$ transitions to only the $0^+$ and $2^+$ states, along with the $\beta$ branching log*ft* of 8.6 indicating a first-forbidden transition to this state. This level is not likely to be the $2^+$ state of the three-phonon multiplet, since the existence of a transition to the ground state violates the selection rule of forbidden three-phonon transitions. The remaining choices are: (1) a two-quasiparticle state, (2) a single-particle state arising from

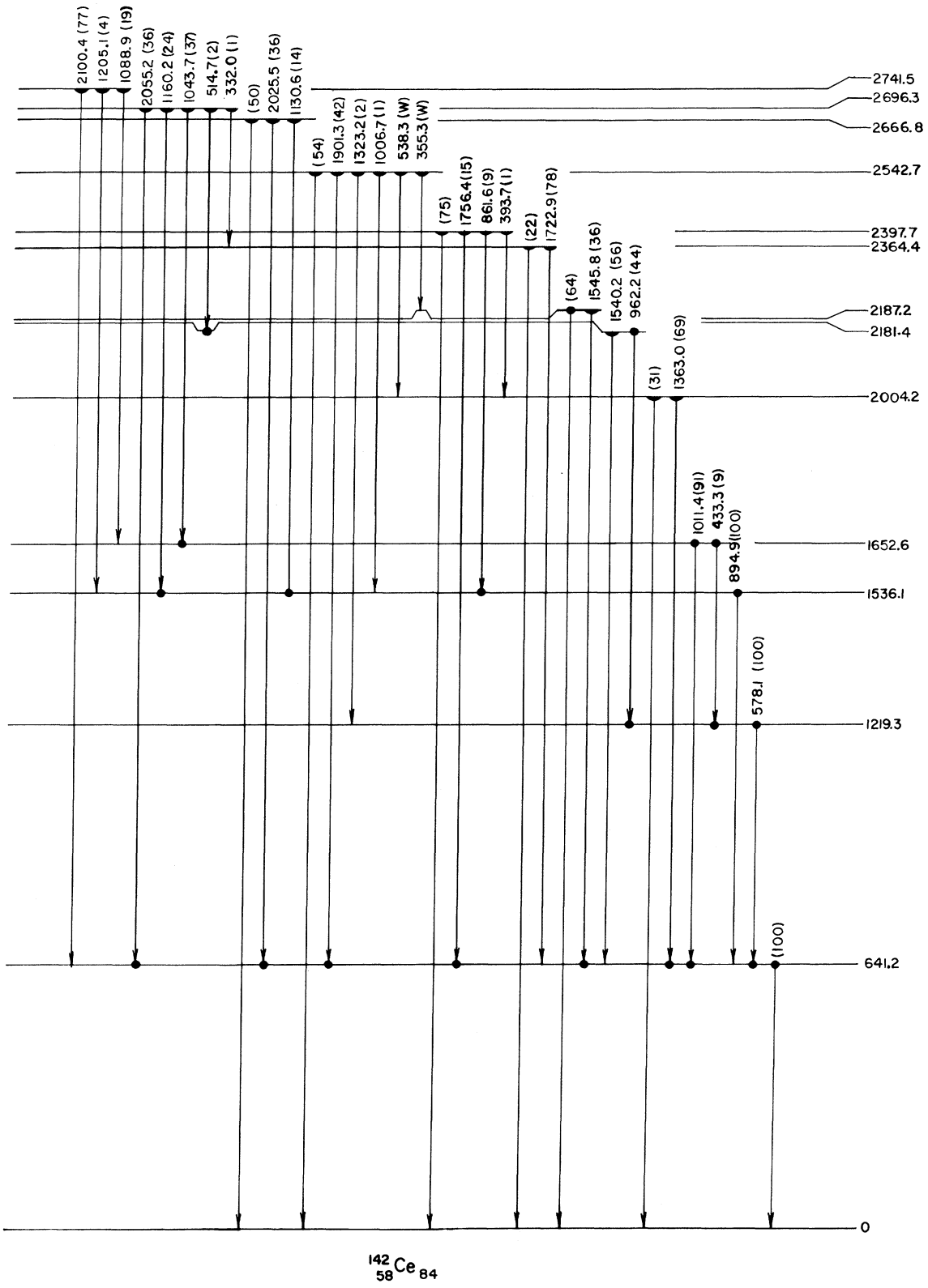


FIG. 6. Low-energy level scheme for $Ce^{142}$.

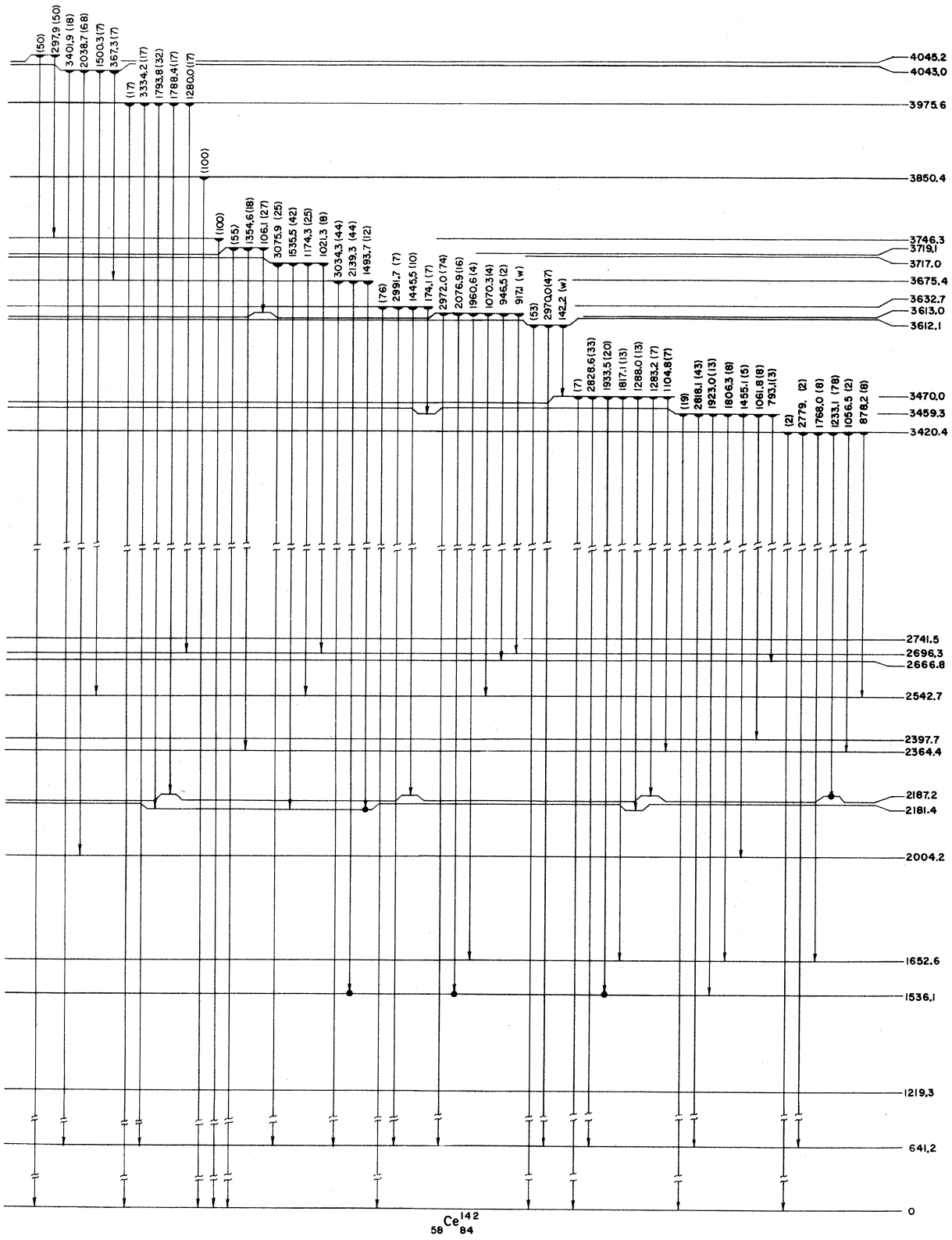


FIG. 7. High-energy level scheme for $Ce^{142}$.

TABLE VII. Calculated log$ft$ values for the decay of $Ba^{142}$.

| $La^{142}$ level (keV) | $E_\beta$ (MeV) | $\beta$ branching (%) | Log$ft$ |
|---|---|---|---|
| 0 | 1.88[a] | 0[b] | |
| 77.6 | 1.80 | 6 | 6.6 |
| 147.0 | | ~0 | |
| 154.6 | 1.73 | 0.1 | 8.3 |
| 255.1 | 1.63 | 1.8 | 6.9 |
| 300.2 | 1.58 | 0.2 | 7.8 |
| 309.0 | 1.57 | 0.8 | 7.2 |
| 334.8 | | ~0 | |
| 361.5 | | ~0 | |
| 363.8 | 1.52 | 1.4 | 6.9 |
| 425.0 | 1.46 | 5.1 | 6.3 |
| 432.3 | 1.45 | 3.5 | 6.4 |
| 590.7 | 1.29 | 0.4 | 7.2 |
| 604.2 | | ~0 | |
| 792.2 | 1.09 | 0.8 | 6.6 |
| 818.2 | 1.06 | 0.3 | 7.0 |
| 867.0 | 1.01 | 0.5 | 6.7 |
| 1078.5 | 0.80 | 20 | 4.7 |
| 1204.1 | 0.68 | 45 | 4.1 |
| 1283.4 | 0.60 | 0.1 | 6.6 |
| 1457.5 | 0.42 | 14 | 3.9 |

[a]From Garvey *et al.* (see Ref. 28).
[b]Assumed to be negligible (see text).

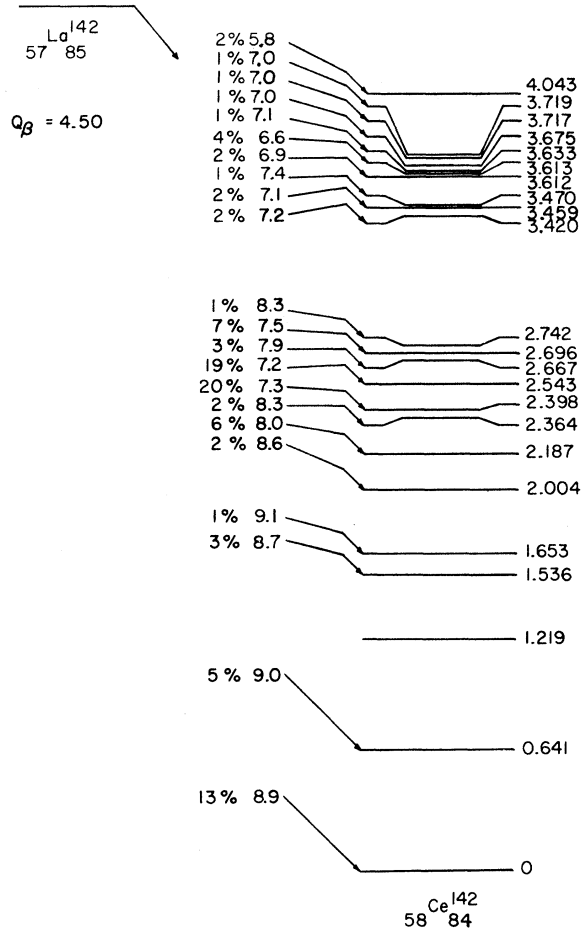


FIG. 8. $\beta$-decay branching percentages and log$ft$ values for $La^{142}$ decay.

some configuration mixing of the proton $g_{7/2}$ and $d_{5/2}$ levels, and (3) some higher-order residual interactions such as pairing-plus-quadrupole or rotation-particle coupling.

A large $\beta$ feeding (20%) is observed to the 2398-keV level; the log$ft$ value (7.3) indicates that this is possibly an allowed transition. Hence an assignment of $J^\pi = 1^-$ is tentatively made, which is supported by the observation of deexcitations only to levels with $J^\pi = 0^+$ or $2^+$. Earlier investigations have an assignment for this state of $2^+$, but the $4^+$ level at 1219 keV, to which no transition is observed from the 2398-keV level in this work, was not previously seen, which leads to a logical choice of $2^+$ supported by a different interpretation of the comparative half-life for $\beta$ feeding to this level.[9,10] Under the present assignment, this state may result from a collective motion or from a quasiparticle excitation in a deformed nucleus. If this $1^-$ state is a four-quasiparticle state and the first $2^+$ state and the $0^+$ ground state are the two-quasiparticle and vacuum-quasiparticle states, respectively, the hindrance for $\gamma$ transitions would be stronger for the $1^- \rightarrow 0^+$ transition than for the $1^- \rightarrow 2^+$ transition. This is compatible with the experimental observation for a number of nearby rare-earth nuclides. In the $Ce^{142}$ nucleus, the ratio of reduced transition probabilities is

$$\frac{B(E1;\ 1^- \rightarrow 2^+)}{B(E1;\ 1^- \rightarrow 0^+)} = 0.52 \pm 0.12,$$

which agrees with other rare-earth nuclei. In the rotational model, if $K=0$ the ratio is 2; if $K=1$ the ratio is $\frac{1}{2}$.[35] It is also not likely that this level is a two-quasiparticle state, because the proton or neutron orbits in the same major shell cannot couple to each other to produce the $1^-$ state unless an energetically unlikely excitation to an orbit in the next major shell occurs. However, if the core is deformed, the orbits will be split in a spheroidal potential and the state can be explained as a two-quasiparticle state with a deformed shape. It is the existence of this state that indicates the "spherical" nucleus may be deformed for a high excitation energy because of the breaking of the pairing force which tends to stabilize the spherical shape of the nucleus.

The next level at 2543 keV is assigned as $J^\pi = 2^+$. This choice is based on the presence of transitions

TABLE VIII. $\gamma$-ray transitions in $Ce^{142}$.

| Energy (keV) | Relative intensity [a] | Energy (keV) | Relative intensity [a] | Energy (keV) | Relative intensity [a] | Energy (keV) | Relative intensity [a] |
|---|---|---|---|---|---|---|---|
| 106.1 ±0.4 | 3±2 | 1061.8 ±0.2 | 3±2 | 1618.2 ±0.2 | 6±2 | 2539.4 ±0.5 | 15±3 |
| 119.4 ±0.6 | <1±1 | 1070.3 ±0.3 | 3±2 | 1651.4 ±0.3 | 4±2 | 2542.65±0.09 | 214±27 |
| 142.2 ±0.6 | <1±1 | 1074.2 ±0.3 | 2±1 | 1688.1 ±0.3 | 5±2 | 2663.5 ±0.3 | 15±3 |
| 169.5 ±0.7 | <1±1 | 1088.9 ±0.15 | 5±2 | 1722.9 ±0.15 | 32±5 | 2666.8 ±0.15 | 36±5 |
| 174.1 ±0.4 | 2±1 | 1100.1 ±0.5 | 1±1 | 1752.4 ±0.7 | 2±1 | 2672.6 ±0.4 | 4±2 |
| 297.9 ±0.3 | 1±1 | 1104.8 ±0.5 | 1±1 | 1756.42±0.07 | 63±9 | 2779 ±1 | 1±1 |
| 332.0 ±0.3 | 1±1 | 1112.6 ±0.3 | 2±1 | 1768.0 ±0.5 | 4±2 | 2782.3 ±0.4 | 6±2 |
| 353.6 ±0.6 | <1±1 | 1116.7 ±0.3 | 2±1 | 1771.0 ±0.5 | 4±2 | 2800.8 ±0.4 | 12±3 |
| 355.3 ±0.8 | <1±1 | 1130.6 ±0.15 | 10±3 | 1778.4 ±0.7 | 1±1 | 2818.10±0.10 | 16±4 |
| 367.3 ±0.2 | 2±1 | 1144.5 ±0.2 | 3±2 | 1793.8 ±0.8 | 2±1 | 2828.6 ±0.2 [d] | 5±2 |
| 393.7 ±0.3 | 2±1 | 1160.16±0.06 | 37±5 | 1806.3 ±0.5 | 3±2 | 2970.0 ±0.7 | 15±3 |
| 408.4 ±0.4 | 1±1 | 1174.3 ±0.3 | 3±2 | 1817.1 ±0.6 | 2±1 | 2972.0 ±0.2 | 63±6 |
| 420.8 ±0.1 | 5±2 | 1190.9 ±0.15 | 8±3 | 1885.4 ±0.7 | 11±3 | 2991.7 ±0.5 | 2±1 |
| 427.9 ±0.5 | 1±1 | 1205.1 ±0.5 | 1±1 | 1901.32±0.08 | 166±11 | 2999.9 ±0.2 | 10±3 |
| 433.34±0.07 [b] | 8±3 | 1231.5 ±0.5 | 6±2 | 1923.0 ±0.3 | 5±2 | 3007.1 ±0.5 | 4±2 |
| 514.7 ±0.3 | 3±2 | 1233.11±0.08 | 39±6 | 1933.5 ±0.5 | 3±2 | 3012.9 ±0.2 | 14±3 |
| 532.0 ±0.2 | 3±2 | 1242.3 ±0.3 | 4±2 | 1948.2 ±0.4 [d] | 10±3 | 3022.3 ±0.7 | 2±1 |
| 538.3 ±0.5 | 1±1 | 1264.7 ±0.3 | 2±1 | 1954 ±1 | 1±1 | 3034.3 ±0.2 | 11±3 |
| 545.8 ±0.7 | <1±1 | 1270.1 ±0.4 | 2±1 | 1960.6 ±0.5 | 3±2 | 3046.9 ±0.2 | 8±3 |
| 571.6 ±0.5 | 1±1 | 1280 ±1 | 1±1 | 2004.2 ±0.15 | 20±4 | 3075.9 ±0.3 | 3±2 |
| 578.09±0.04 | 26±4 | 1283.2 ±0.5 | 1±1 | 2025.5 ±0.14 | 26±4 | 3155.0 ±0.3 | 4±2 |
| 597.6 ±0.5 | 1±1 | 1288.0 ±0.3 | 2±1 | 2038.7 ±0.2 | 21±4 | 3181.0 ±0.3 | 6±2 |
| 601.8 ±0.5 | 1±1 | 1323.2 ±0.2 | 7±2 | 2050.4 ±0.2 | 10±3 | 3236.7 ±0.2 | 6±2 |
| 619.5 ±0.10 | 3±1 | 1332.3 ±0.4 | 2±1 | 2055.17±0.07 | 56±6 | 3242.4 ±0.3 | 4±2 |
| 641.17±0.03 | 1000±87 | 1341.2 ±0.6 | 1±1 | 2076.9 ±0.2 | 14±3 | 3273.2 ±0.7 | 3±2 |
| 793.1 ±0.4 | 1±1 | 1354.6 ±0.5 | 2±1 | 2086.1 ±0.2 | 8±3 | 3314.7 ±0.2 | 26±4 |
| 861.57±0.07 | 38±6 | 1362.95±0.05 | 45±6 | 2100.4 ±0.2 | 20±4 | 3334.2 ±0.7 | 1±1 |
| 878.2 ±0.3 | 4±2 | 1373.6 ±0.7 | 4±2 | 2126.2 ±0.3 | 7±3 | 3401.9 ±0.3 | 6±2 |
| 894.85±0.04 [b] | 179±20 | 1389.3 ±0.1 [c] | 9±3 | 2139.3 ±0.2 | 11±3 | 3420.4 ±0.4 | 1±1 |
| 917.1 ±0.5 | 1±1 | 1395.3 ±0.2 | 4±2 | 2180.3 ±0.2 | 11±3 | 3459.3 ±0.2 | 7±3 |
| 946.5 ±0.3 | 2±1 | 1402.2 ±0.2 | 3±2 | 2187.2 ±0.1 | 111±14 | 3470.0 ±0.5 | 1±1 |
| 962.2 ±0.13 | 8±3 | 1445.5 ±0.3 | 3±2 | 2290.5 ±0.6 | 7±3 | 3612.1 ±0.2 | 17±4 |
| 991.2 ±0.3 | 2±1 | 1455.1 ±0.3 | 2±1 | 2358.4 ±0.2 | 16±3 | 3632.7 ±0.2 | 22±4 |
| 1006.7 ±0.2 | 5±2 | 1493.7 ±0.2 [c] | 3±2 | 2364.4 ±0.3 | 9±3 | 3719.1 ±0.2 | 6±2 |
| 1011.38±0.06 | 83±10 | 1500.3 ±0.5 | 2±1 | 2397.72±0.10 | 313±33 | 3746.3 ±0.8 | 1±1 |
| 1021.3 ±0.7 | 1±1 | 1516.3 ±0.2 | 9±3 | 2419.5 ±0.4 | 4±2 | 3850.4 ±0.3 | 5±2 |
| 1039.2 ±0.3 | 2±1 | 1535.5 ±0.3 | 5±2 | 2459.4 ±0.4 [c] | 8±3 | 3975.6 ±0.2 | 1±1 |
| 1043.68±0.07 | 58±7 | 1540.2 ±0.15 | 10±3 | 2513.2 ±0.6 | 3±2 | 4045.2 ±0.3 | 1±1 |
| 1056.5 ±0.4 | 1±1 | 1545.8 ±0.1 | 63±9 | 2532.3 ±0.7 | 2±1 | | |

[a] Measured relative to the 641.2-keV transition.

[b] A similar energy transition occurs in $La^{142}$.

[c] A single-escape peak is also found at this energy.

[d] A double-escape peak is also found at this energy.

to the $0^+$, $2^+$, and $4^+$ states. The log$ft$ of 7.2 for the $\beta$ branch feeding this state may suggest a first-forbidden transition, which is consistent with the level assignment.

The final level to be interpreted is at 3459 keV. This level has a possible $J^\pi$ of either $2^+$ or $1^-$ primarily because of observed transitions to the $0^+$, $2^+$, and $3^-$ states. The comparative half-life value of 7.1 might indicate an allowed transition, but such a choice is not clear because of the relatively small branching ratio observed (2%) and associated errors from $\gamma$ intensity balances. The lack of observational data on the transitions from the high-spin members of the different $K$ bands handicaps the interpretation of the nuclide with regard to the collective-model limits. Application of the variable-moment-of-inertia model[23] cannot be done for this case, since the present model requires $E(4^+)/E(2^+) \geq 2.23$.

The above discussion about the nature of $Ce^{142}$ has been carried out with the implicit assumption that all of the important $\gamma$-ray transitions have multipolarity of $E1$ or $E2$. In reality, this is not the case, as appreciable admixtures of $M1$ multi-

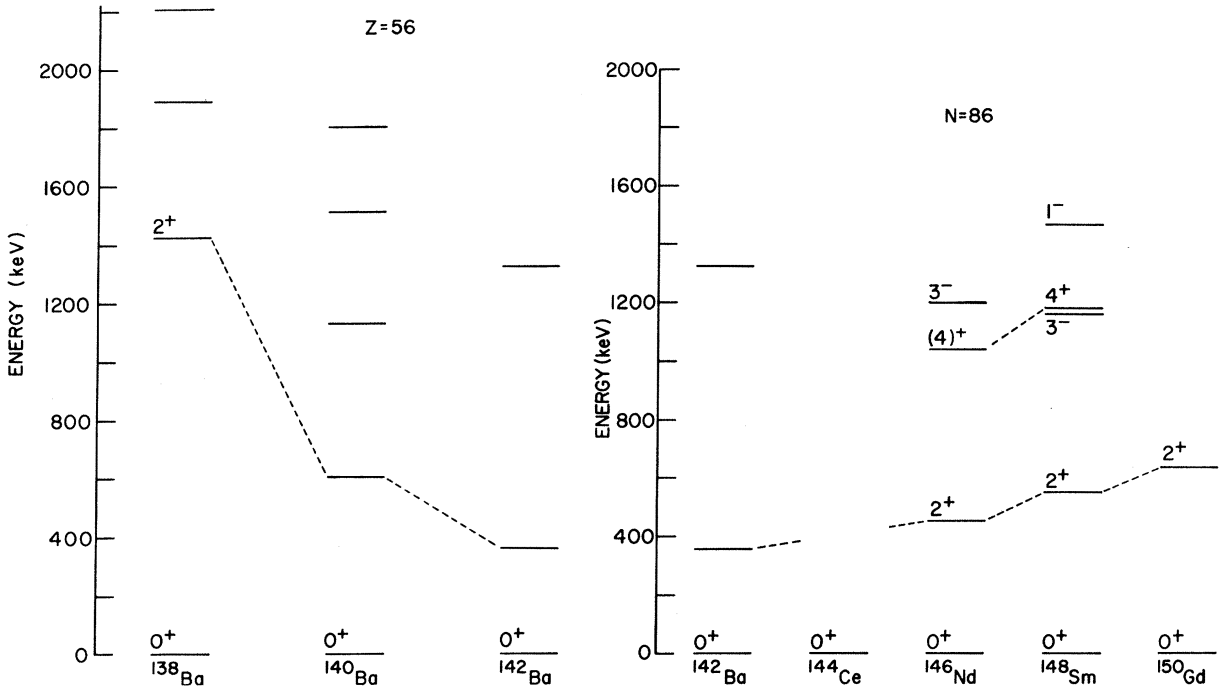


FIG. 9. The lower-energy levels of the $Z=56$ and $N=86$ nuclides; $Ce^{144}$ has not been investigated.

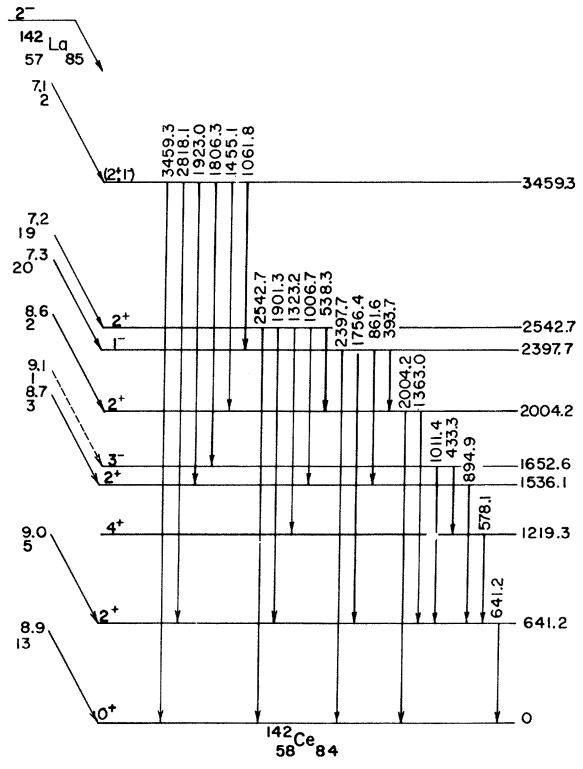


FIG. 10. The significant energy levels and $\beta$ branching for $Ce^{142}$, showing the spin assignments based on the present work.

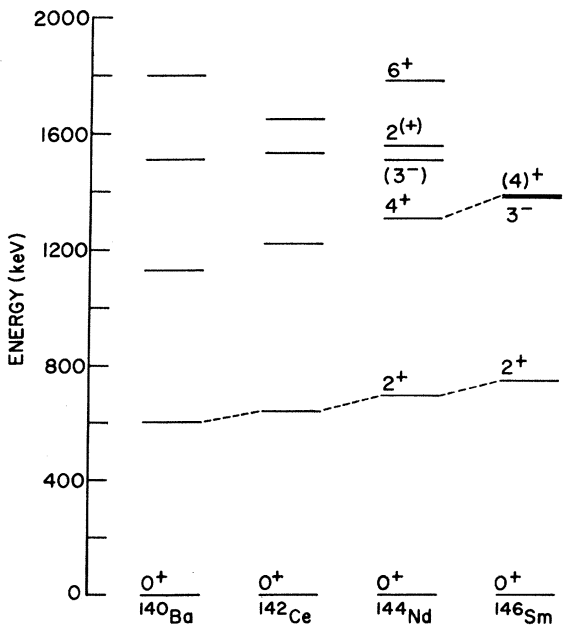


FIG. 11. The lower-energy levels of the $N=84$ nuclides.

TABLE IX. $\gamma$-ray coincidences in $Ce^{142}$.

| Gating transition (keV) | Coincidence transitions (keV) |
|---|---|
| 433.3 | 578.1, 641.2 |
| 578.1 | 433.3, 641.2, 962.2, 1043.7, 1493.7 |
| 641.2 | 433.3, 514.7, 578.1, 861.6, 894.9, 1011.4, 1043.7, 1130.6, 1160.2, 1233.1, 1363.0, 1545.8, 1722.9, 1756.4, 1901.3, 1933.5, 2025.5, 2038.7 (?), 2055.2 |
| 861.6 | 641.2, 894.9 |
| 894.9 | 641.2, 861.6, 1160.2, 2076.9, 2139.3 |
| 1011.4 | 641.2, 1043.7 |
| 1043.7 | 433.3, 578.1, 641.2, 1011.4 |
| 1130.6 | 641.2, 894.9 |
| 1160.2 | 641.2, 894.9 |
| 1233.1 | 641.2, 1545.8, 2187.2 |
| 1363.0 | 641.2 |
| 1545.8 | 641.2, 1233.1 |
| 1722.9 | 641.2 |
| 1756.4 | 641.2 |
| 1901.3 | 641.2 |
| 1933.5 | 641.2, 894.9 (?) |
| 2187.2 | 1233.1 |

TABLE X. Calculated log$ft$ values for the decay of $La^{142}$.

| $Ce^{142}$ level (keV) | $E$ (MeV) | $\beta$ branching (%) | Log$ft$ |
|---|---|---|---|
| 0 | 4.50 [a] | 13 [b] | 8.9 |
| 641.2 | 3.86 | 5 | 9.0 |
| 1219.3 | | ~0 | |
| 1536.1 | 2.96 | 3 | 8.7 |
| 1652.6 | 2.85 | 1 | 9.1 |
| 2004.2 | 2.50 | 2 | 8.6 |
| 2181.4 | | ~0 | |
| 2187.2 | 2.31 | 6 | 8.0 |
| 2364.4 | 2.14 | 2 | 8.3 |
| 2397.7 | 2.10 | 20 | 7.3 |
| 2542.7 | 1.96 | 19 | 7.2 |
| 2666.8 | 1.83 | 3 | 7.9 |
| 2696.3 | 1.80 | 7 | 7.5 |
| 2741.5 | 1.76 | 1 | 8.3 |
| 3420.4 | 1.08 | 2 | 7.2 |
| 3459.3 | 1.04 | 2 | 7.1 |
| 3470.0 | 1.03 | 1 | 7.4 |
| 3612.1 | 0.89 | 2 | 6.9 |
| 3613.0 | 0.89 | 4 | 6.6 |
| 3632.7 | 0.87 | 1 | 7.1 |
| 3675.4 | 0.83 | 1 | 7.0 |
| 3717.0 | 0.78 | 1 | 7.0 |
| 3719.1 | 0.78 | 1 | 7.0 |
| 3746.3 | | ~0 | |
| 3850.4 | | ~0 | |
| 3975.6 | | ~0 | |
| 4043.0 | 0.46 | 2 | 5.8 |
| 4045.2 | | 0 | |

[a] From Ref. 28.
[b] From Ref. 9.

polarity are often seen together with $E2$ transitions for deexcitations from the higher-phonon or single-particle states.

## VI. CONCLUSIONS

It is evident that more experimental information is needed for all four nuclei to establish the nature of the individual levels. In addition to possible refinement and extension of the measurements reported here, studies of the $\beta$-decay modes, internal-conversion processes, and directional correlations are needed.

A precise explanation of the character of these nuclei is not possible at present. These initial studies reveal that the $Ce^{142}$ nucleus is primarily vibrational in character with little evidence of rotational properties. However, the very crude results for the even-even $Ba^{142}$ nucleus suggest quite a different character. It would not be unrealistic to ascribe this behavior to the onset of a different interaction becoming important as the $N = 88$ to 90 gap is approached. It is also conceivable to suggest that some shape isomerism appears at higher-energy levels in these transitional nuclei.

## ACKNOWLEDGMENTS

The authors would like to express their thanks to K. L. Malaby for his assistance in performing the chemical separations for the La activities, and to Dr. W. C. Schick, Jr., for his assistance in computation and stimulating discussions.

†Work was performed in the Ames Laboratory of the U. S. Atomic Energy Commission (contribution No. 2861).

*Present address: Lawrence Radiation Laboratory, Livermore, California.

[1]W. L. Talbert, Jr., and D. Thomas, Nucl. Instr. Methods 38, 306 (1965).

[2]W. L. Talbert, Jr., and J. R. McConnell, Arkiv Fysik 36, 99 (1967).

[3]G. H. Carlson, W. C. Schick, Jr., W. L. Talbert, Jr., and F. K. Wohn, Nucl. Phys. A125, 267 (1969).

[4]W. L. Talbert, Jr., A. B. Tucker, and G. M. Day, Phys. Rev. 177, 1805 (1969).

[5]T. Alvager, R. A. Naumann, R. F. Petry, G. Sidenius, and T. D. Thomas, Phys. Rev. 167, 1105 (1968).

[6]K. Fritze and T. J. Kennett, Phys. Rev. 127, 1262 (1962).

[7]R. P. Schuman, E. H. Turk, and R. L. Heath, Phys. Rev. 115, 185 (1959).

[8]R. J. Bullock and N. R. Large, Atomic Energy Research Establishment (Harwell, Berkshire) Report No. AERE-R 5568, 1968 (unpublished).

[9]W. V. Prestwich and T. J. Kennett, Phys. Rev. 134, B485 (1964).

[10]W. V. Prestwich and T. J. Kennett, Nucl. Phys. 67, 302 (1965).

[11]Revised $A$ chains, $A$=142, Nucl. Data B2, No. 1,1 (1967).

[12]C. M. Lederer, J. M. Hollander, and I. Perlman, *Table of Isotopes* (John Wiley & Sons, Inc., New York, 1967), 6th ed.

[13]L. S. Kisslinger and R. A. Sorenson, Rev. Mod. Phys. 35, 853 (1963).

[14]G. Scharff-Goldhaber, J. Phys. Soc. Japan Suppl. 24, 150 (1968).

[15]R. A. Sorenson, in *Proceedings of the International Conference on Properties of Nuclear States, Montréal, Canada, 1969* (Les Presses de l'Université de Montréal, Montréal, Canada, 1969), p. 85.

[16]K. Kumar and M. Baranger, Nucl. Phys. A92, 608 (1967).

[17]K. Kumar, Nucl. Phys. A92, 653 (1967).

[18]M. Baranger and K. Kumar, Nucl. Phys. A110, 490 (1968).

[19]K. Kumar and M. Baranger, Nucl. Phys. A110, 529 (1968).

[20]K. Kumar and M. Baranger, Nucl. Phys. A122, 241 (1968).

[21]K. Kumar and M. Baranger, Phys. Rev. Letters 17, 1146 (1966).

[22]K. Kumar and M. Baranger, Nucl. Phys. A122, 273 (1968).

[23]M. A. J. Mariscotti, G. Scharff-Goldhaber, and B. Buck, Phys. Rev. 178, 1864 (1969).

[24]T. Marumori, M. Yamanura, Y. Miyanisui, and S. Nishiyama, in *Proceedings of the International Conference on Properties of Nuclear States, Montréal, Canada, 1969* (Les Presses de l'Université de Montréal, Montréal, Canada, 1969), p. 103.

[25]R. M. Dreizler and A. Klein, Phys. Letters 30B, 236 (1969).

[26]A. C. Wahl, R. L. Ferguson, D. R. Nethaway, D. E. Troutner, and Z. K. Wolfsberg, Phys. Rev. 126, 1112 (1962).

[27]J. H. Norman, W. L. Talbert, Jr., and D. M. Roberts, U. S. Atomic Energy Commission Report No. IS-1893, Iowa State University, 1968 (unpublished).

[28]G. T. Garvey, W. J. Gerace, R. L. Jaffe, I. Talmi, and I. Kelson, Rev. Mod. Phys. 41, 1 (1969).

[29]L. A. Sliv and I. M. Band, in *Alpha-, Beta-, and Gamma-ray Spectroscopy*, edited by K. Siegbahn (North-Holland Publishing Company, Amsterdam, The Netherlands, 1965), Vol. II.

[30]Y. K. Agarwal, C. V. K. Baba, and S. K. Bhattacherjee, Nucl. Phys. 58, 641 (1964).

[31]N. B. Gove, in *Nuclear Spin-Parity Assignments*, edited by N. B. Gove and R. L. Robinson (Academic Press Inc., New York, 1966).

[32]W. C. Schick, Jr., private communication.

[33]A. S. Davydov and G. F. Filippov, Nucl. Phys. 8, 237 (1958).

[34]M. Guttman, E. G. Funk, and J. W. Mihelich, Nucl. Phys. 64, 401 (1964).

[35]M. Sakai, Phys. Letters 3, 338 (1963).